ADVANCES IN ATMOSPHERIC SCIENCES, VOL. 31, JULY 2014, 985–994

The Role of Atmospheric Teleconnection in the Subtropical Thermal Forcing on the Equatorial Pacific

WANG Lu*[1,2] and YANG Haijun[2]

[1]*Nuclear and Radiation Safety Center, Ministry of Environmental Protection of the People's Republic of China, Beijing* 100082
[2]*Laboratory for Climate and Ocean–Atmosphere Studies and the Department of Atmospheric and Oceanic Sciences, Peking University, Beijing* 100871

(Received 2 September 2013; revised 20 November 2013; accepted 27 December 2013)

ABSTRACT

The equatorial response to subtropical Pacific forcing was studied in a coupled climate model. The forcings in the western, central and eastern subtropical Pacific all caused a significant response in the equatorial thermocline, with comparable magnitudes. This work highlights the key role of air–sea coupling in the subtropical impact on the equatorial thermocline, instead of only the role of the "oceanic tunnel". The suggested mechanism is that the cyclonic (anticyclonic) circulation in the atmosphere caused by the subtropical surface warming (cooling) can generate an anomalous upwelling (downwelling) in the interior region. At the same time, an anomalous downwelling (upwelling) occurs at the equatorward flank of the forcing, which produces anomalous thermocline warming (cooling), propagating equatorward and resulting in warming (cooling) in the equatorial thermocline. This is an indirect process that is much faster than the "oceanic tunnel" mechanism in the subtropical impact on the equator.

Key words: subtropical Pacific, upwelling, downwelling, equatorial thermocline

Citation: Wang, L., and H. J. Yang, 2014: The role of atmospheric teleconnection in the subtropical thermal forcing on the equatorial Pacific. *Adv. Atmos. Sci.*, **31**(4), 985–994, doi: 10.1007/s00376-013-3173-1.

1. Introduction

There have been many studies on the interaction between the subtropics and tropics that have focused on subtropical–equatorial exchanges of water. In a zonally integrated sense, the water exchange within the tropical Pacific can be described in terms of shallow subtropical–tropical overturning cells (STCs) (Liu et al., 1994; McCreary and Lu, 1994), involving equatorward geostrophic transport within the main thermocline, upwelling at the equator, and returning surface Ekman flow to the subtropics.

Observations as well as modelling studies have improved knowledge regarding the routes, strength, mechanisms and variations of the subtropical–tropical thermocline water pathways (i.e. the subsurface branches of the Pacific STCs), through which waters within the subtropics flow into the equatorial Pacific Ocean (e.g. McPhaden and Fine, 1988; Liu et al., 1994; McCreary and Lu, 1994; Gu and Philander, 1997; Rothstein et al., 1998; Huang and Liu, 1999; Coles and Rienecker, 2001; Huang and Wang, 2001; Lee and Fukumori, 2003; Wang and Huang, 2005). A common feature is that pycnocline water, which is subducted in the central and eastern subtropical Pacific, flows westward and equatorward into the equatorial Pacific Ocean either through the low-latitude western boundary current (LLWBC) or through the interior ocean, finally joining the equatorial undercurrent (Gu and Philander, 1997). Using the National Centers for Environmental Prediction's (NCEP's) ocean GCM, in which observed temperatures are assimilated, Huang and Liu (1999) showed that the equatorward LLWBC and interior transports are about 14 and 3 Sv, respectively, at 10°N. Potential vorticity dynamics are crucial for explaining the routes taken by subtropical thermocline waters as they intrude into the tropics (Rothstein et al., 1998), as well as the changes in their transport under global warming (Luo et al., 2009). The variability of the boundary and interior pathways have also been extensively investigated. By examining the interannual variability of interior transport, Huang and Wang (2001) found signals associated with the El Niño–Southern Oscillation (ENSO). It has also been noticed that interior exchange has a seasonal cycle related to the seasonality of pycnocline thickness because of the seasonal variability of local Ekman pumping (Coles and Rienecker, 2001).

It is believed that the passive tracers released in the western subtropical North Pacific cannot reach the equator by Lagrangian trajectory simulations (e.g. Huang and Liu, 1999). This region is a so-called "recirculation window" (RW),

* Corresponding author: WANG Lu
Email: wanglu@chinansc.cn

within which the subducted waters recirculate in the subtropical ocean itself (Huang and Liu, 1999). Less is known about the impact of the thermal forcing in the western subtropical Pacific on the equatorial climate, especially on the thermocline. In a recent coupled GCM study (Matei et al., 2008), the relative impact of the subtropical North and South Pacific oceans on the tropical Pacific climate mean state and variability was quantified using tailored experiments in which the model was forced by idealized SST anomalies in the subtropics of both hemispheres. In their experiments, a 2°C warming/cooling was applied in the uppermost layer of the selected domains, which were both in the regions of subduction windows as indicated by Liu et al. (1994), Gu and Philander (1997), and Huang and Liu (1999). Outside those domains they allowed full ocean–atmosphere coupling. The model results suggested that the subtropics affect equatorial climate mainly through a slow "oceanic tunnel" in the North Pacific Ocean. Nevertheless, the impact of western subtropical North Pacific thermal forcing on the equator remains unclear. There are two questions that interest us the most: (1) Can the western subtropical North Pacific thermal forcing impact on the equatorial climate, especially the thermocline? (2) If so, what are the mechanisms by which the thermal forcing in the western, central and eastern subtropics impact on the equatorial mean climate?

This work complements our recent study (Wang and Yang, 2013), in which we investigated the impact of subtropical Pacific sea surface temperature anomalies (SSTAs) on the equatorial ocean, but did not discuss the possible mechanisms in detail. In that previous work, we proposed that a "wind–evaporation–SST" mechanism plays the dominant role in equatorial SST changes; while in this work, we propose that air–sea coupling, which is much faster than the "oceanic tunnel", plays the dominant role in the process of subtropical SSTA impact on the equatorial thermocline. The mechanisms were investigated in detail in the present study through the approach of term balance analyses.

Using a so-called "partial coupling" (PC) technique in a fully coupled climate model, sensitivity experiments were carried out with localized SST warming over different longitude bands in the subtropical North Pacific. Although the prescribed SST warming in the subtropics was found to be well beyond the range of intrinsic coupled variability, it was within the range of the SST change for a doubling of CO_2 (Kerr, 2004). The strong anomaly is necessary for generating significant change in this remote region. Our results indicate that the impacts of the SSTAs in different longitude bands within the subtropical North Pacific on the equatorial thermocline are comparable, with the warming from off-equator anomalous downwelling areas playing the dominant role. Instead of focusing on the oceanic tunnel, in this study we emphasize that air–sea coupling plays an indirect but efficient role in the equatorward propagation of the subtropical thermal forcing.

All the results presented in this paper are appropriate for our model, but could be model-dependent. However, we expect that the physical processes demonstrated here and our understanding of climate adjustment to remote forcing could be helpful to understand the reality. A more complete description of the sensitivity experiments is given in section 2. Section 3 describes the thermocline responses in the equatorial Pacific. Section 4 investigates the possible mechanisms underpinning the equatorial thermocline responses. And finally, a summary and discussion are presented in section 5.

2. Model, experiments and methods

The model used in this study was the Fast Ocean–Atmosphere Model (FOAM), developed jointly at the University of Wisconsin–Madison and the Argonne National Laboratory (Jacob, 1997). More details about the model can be found, for example, in Yang and Liu (2005), and Yang and Wang (2011).

To quantify the impact of the climate change within one region on the climate in another remote region, the PC technique was used in FOAM. Using this approach, the full air–sea coupling in a selected region was mandatorily suppressed, with an anomalous signal forcing the model atmosphere or ocean. Full coupling was kept unchanged everywhere else.

Using the same modelling technique as in Yang and Wang (2011), we performed three pairs of PC experiments to explicitly quantify the sensitivity of the equator to thermal forcing in the subtropical North Pacific. All experiments started from a stable control run (CTRL) and were integrated for 200 years, when the upper ocean had reached quasi-equilibrium. In the PC experiments, a 2°C SST warming (cooling) was "seen" by both the atmosphere and ocean in the western (105°–160°E), central (160°E–160°W), and eastern (160°–105°W) subtropical Pacific between 20°–30°N, respectively (Fig. 1, solid line rectangular boxes). These experiments are referred to as WSP, CSP and ESP hereafter. For each sensitivity experiment, the ocean and atmosphere was partially coupled in the specific domain where the atmosphere was forced by the climatic cycle of heat flux from the CTRL plus anomalous heat flux calculated from the 2°C SST warming, and the ocean was forced by the heat flux from the atmosphere. The atmosphere and ocean remained fully coupled outside the PC region. Each experiment had its own CTRL, in which the PC was still applied in the corresponding domain but without anomalous SST forcing. The impact of the PC forcing was conveyed equatorward by both the atmospheric and oceanic processes. The relative contributions of the western, central, and eastern subtropical Pacific to the equator could be estimated by studying the difference between the sensitivity experiments and corresponding CTRLs. In the following, the equatorial response was calculated as the difference averaged over the last 50 years.

To quantify the contributions of different mechanisms to equatorial changes, we examined the heat budget by calculating the terms in the temperature equation (see Appendix). The term differences between the warming experiments and CTRLs were analyzed.

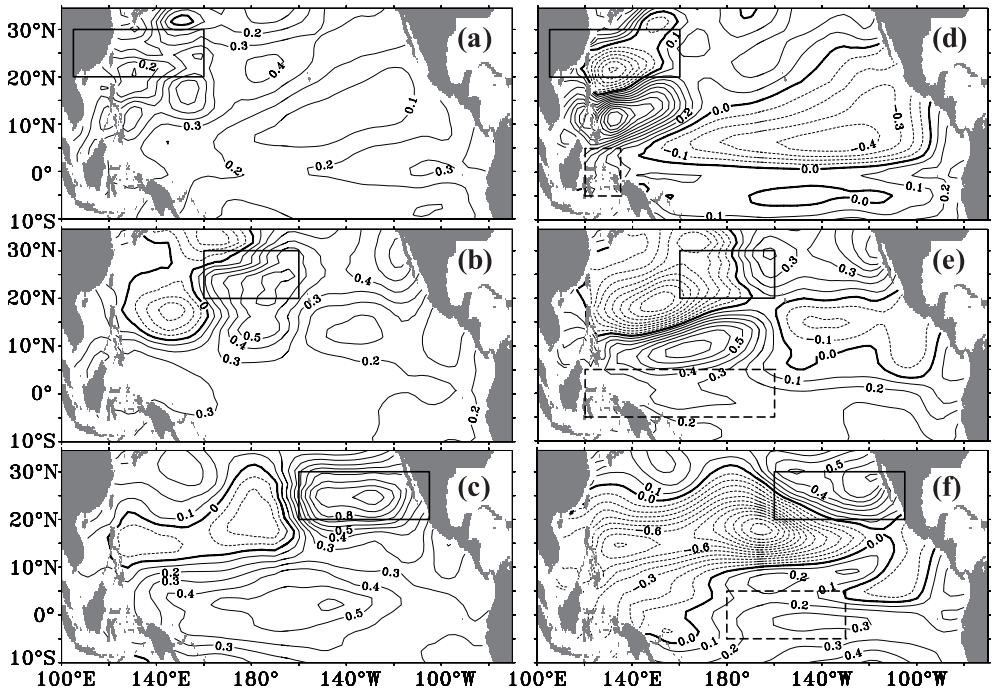

Fig. 1. SSTA (left) and temperature (right) changes in the thermocline (22.7–25.5 isopycnal level) for the (a, d) WSP, (b, e) CSP, and (c, f) ESP experiments averaged over the last 50 years of each run. The subtropical forcing domains are indicated using the solid line rectangular boxes. The dashed line rectangular boxes represent the areas for equatorial heat budget analysis in each case.

3. General impact of the subtropical North Pacific

A 2°C SST warming in WSP, CSP and ESP ultimately increased the equatorial SST by 0.23°C, 0.27°C, and 0.40°C, respectively (Fig. 2, red lines). The equatorial subsurface temperature changes were much weaker than the changes in SST. It was seen that the surface equator responded to the subtropical forcing quickly, and was almost independent of the location of forcing. This implies a significant atmospheric role in the tropical–subtropical interaction. It was also found that the magnitude of the equatorial response increased slightly with the eastward displacement of the subtropical forcing, suggesting thermal forcing in the eastern subtropical Pacific, compared with other longitude bands, is more efficient in terms of the equatorial SST changes it causes. The subsurface responses showed a cooling anomaly during the first couple of decades that were opposite to the surface, suggesting a baroclinic response in the equatorial upper ocean. It also took a much longer time for the subsurface ocean to reach the quasi-equilibrium and the final responses showed a weak warming in general (0.04°C, 0.17°C, and 0.10°C, respectively; Fig. 2, blue lines).

The equatorial responses to subtropical forcings at different locations were actually very different, although the general responses were comparable in magnitude. The horizontal patterns of SST changes showed that the ESP forcing caused the biggest response in the tropics between 10°S and 10°N, in both magnitude and range (Fig. 1c). The equatorial responses to WSP and CSP forcing were more or less concentrated in

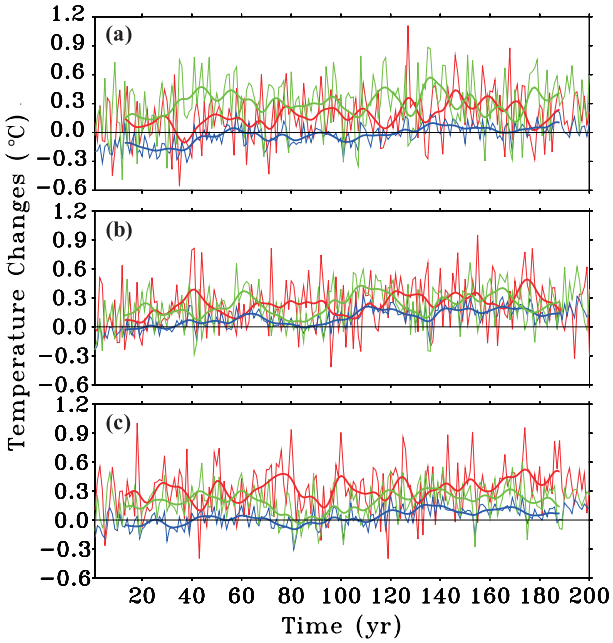

Fig. 2. Time evolution of Pacific temperature changes for the (a) WSP, (b) CSP, and (c) ESP experiments. The red lines and blue lines represent the temperature changes in the equatorial (5°S–5°N, 120°E–80°W) surface (0–40 m) and subsurface (40–400 m), respectively. The green lines represent the temperature changes in the thermocline (22.7–25.5 isopycnal level) within the dashed line rectangular boxes indicated in Figs. 1d, e, and f for each case. The 25-yr running means are also plotted as thick lines.

the west, with comparable amplitude (Figs. 1a and b). The thermocline changes were more dramatically different from the surface. First of all, locally, a clear baroclinic structure was apparent in the subtropical forcing region when compared to the surface (Fig. 1d–f). There were strong coolings beneath the surface warming forcings. This was particularly clear for the WSP and CSP forcings (Figs. 1d and e). In the ESP forcing case, the thermocline cooling was shifted to the southwest of the surface warming (Fig. 1f), with the range extending from 30°N to the equator and from 120°W to the whole western Pacific. Second, remotely, there were strong warming anomalies between 0° and 15°N, induced directly to the south of cooling anomalies in the WSP and CSP forcing cases (Figs. 1d and e). In the ESP forcing, the equatorial thermocline warming was located in the central-eastern part (Fig. 1f). The local off-equatorial warming centers were related to the surface wind forcing, and we prove this in more detail later.

The equatorial warming, no matter whether the centers were on the equator or off-equator, on the surface or at the thermocline, appeared to lack any clear connection with the source forcing regions. This can be clearly seen in the meridional section of the temperature changes (Fig. 3). In WSP and CSP, equatorial thermocline anomalies were isolated from the subtropical SST anomalies by a warming center located at the equatorial flank of the subtropical forcing domains. The warming started from this center, penetrated equatorward through the North Equatorial Counter Current (NECC), and then joined the Southern Equatorial Current (SEC) and Equatorial Undercurrent (EUC) (Fig. 3a, b). In ESP, the warming basically penetrated equatorward through the NECC within a shallower thermocline, and then finally joined the SEC (Fig. 3c).

The zonal sections of equatorial temperature changes show the differences clearly (Fig. 4). For the equilibrium stage (Figs. 4d–f), the warmings concentrated in the west, central-west and central–east under the WSP, CSP and ESP forcings, respectively. It was also found that the warmings were located in the upper thermocline (above 20°C isothermal level), below which there was either cooling or very weak warming. This also explains the generally weak response in the equatorial thermocline shown in Figs. 1d–f. It is interesting to check the transient response along the equator (Figs. 4a–c). During the first 5 years, the equatorial thermocline warming centers were located at the western boundary, western-central part, and central part of the Pacific Ocean basin, respectively. The response patterns resembled the final state very well, with the warming centers being exactly in the locations where they were in equilibrium stages. This implies that a fast atmospheric teleconnection played a role in the equator–off-equator interaction.

4. Mechanisms

In this paper, we pay more attention to the changes in the equatorial thermocline, which are believed to be caused

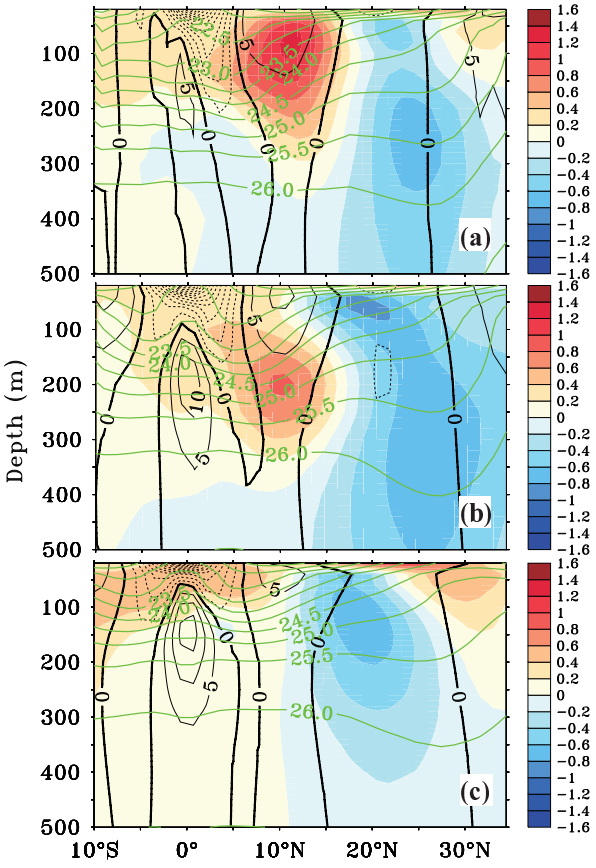

Fig. 3. Zonal averaged temperature changes (colors) in the (a) WSP (120°–150°E), (b) CSP (140°–180°E), and (c) ESP (170°–110°W) experiments. The black contours represent zonal velocity (cm s^{-1}). The green contours represent isopycnal levels (kg m^{-3}). The vertical axis represents depth in the ocean (m).

by the "oceanic tunnel" from the central or eastern subtropical Pacific. If the SST anomalies we exerted in the subtropical North Pacific are treated as passive tracers, both the time scale of the impact of the subtropics on the equatorial thermocline and the changes in the equatorial thermocline can be expected according to the subtropical–equatorial water pathway theory, as demonstrated by previous studies (e.g. Gu and Philander, 1997; Huang and Liu, 1999). It has been pointed out that the time scale of water exchange between the subtropics and equator is decadal to multidecadal. For example, Matei et al. (2008) showed in their North Pacific subduction window thermal forcing experiment that there was no significant temperature change propagating through the oceanic tunnel to the equatorial subsurface until 30 years after the onset of subtropical warming. In addition, the maximum of equatorial thermocline changes for ESP and CSP could be expected to occur at about 140°W, where the NECC merges with the EUC, or at the west boundary where the warm waters join the EUC right after pushing southward along the Mindanao Current. For WSP, the subtropical SST anomalies should not be able to reach the equator because the subducted warm water

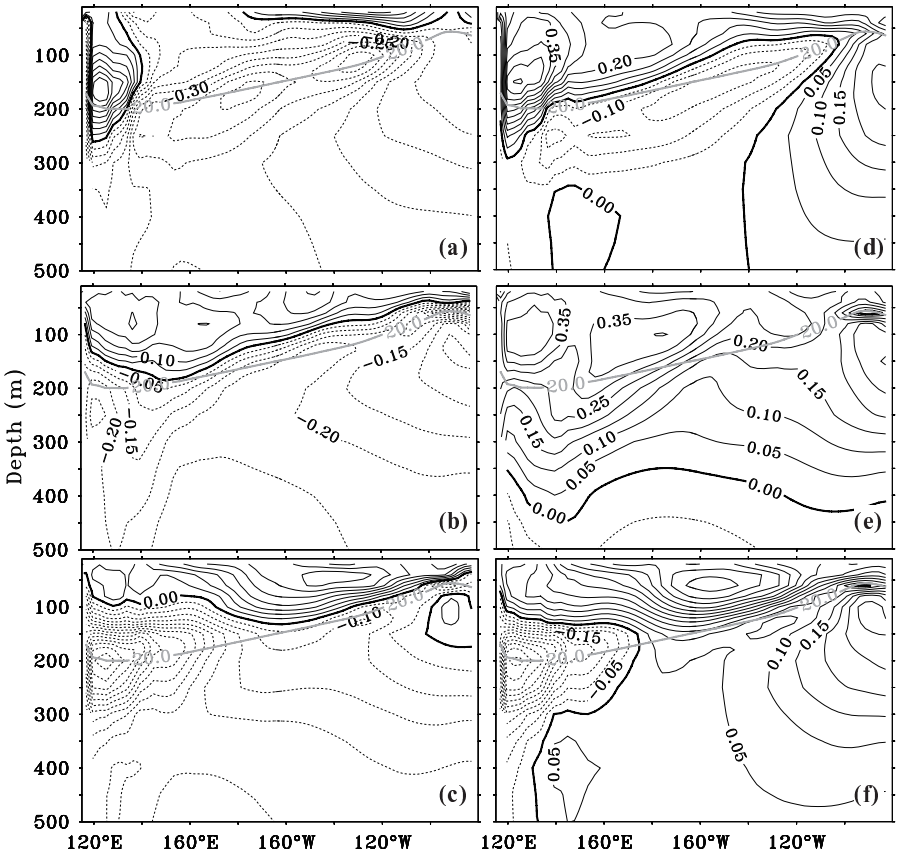

Fig. 4. Temperature changes at the equator (5°S–5°N) in the (a, d) WSP, (b, e) CSP, and (c, f) ESP experiments for the first 5 years (left panel) and the last 50 years (right panel). The grey lines represent the 20°C isotherm in the corresponding CTRL runs. The vertical axis represents depth in the ocean (m).

would be located within the "recirculation window" (Huang and Liu, 1999).

The subtropical North Pacific warming in our experiments, however, seemed not to impact the equatorial thermocline through the pathways of the oceanic tunnel. On the one hand, the first 5-yr averaged response captured maximum warming located in the same position as it was in the final steady state for each sensitivity experiment (Figs. 4a–f), which implies that there should be another process faster than the oceanic tunnel generating the equatorial thermocline warming. On the other hand, for WSP, a strong warming occurred in the western equatorial Pacific within the upper thermocline (Figs. 4a and d), which is inconsistent with the water exchange pathway theory. It is also worth noting that all the maximum warmings in our three sensitivity experiments were within the equatorial upper thermocline (above the 20°C isotherm), which reminds us that these warmings might have come from the lower latitudes instead of the subtropics.

4.1. *Role of atmospheric teleconnection*

We propose that the dipole-like subtropical cooling and the associated warming in the south, which was the reason for the equatorial thermocline warming, resulted from air–sea interaction. The subtropical SST forcing caused anomalous low pressure and cyclonic wind stress locally (Figs. 5a–c), which in turn induced anomalous upwelling at the bottom of the Ekman layer (Figs. 5d–f). The cold water from the bottom of the Ekman layer led to local subsurface cooling. The westward propagation of the baroclinic Rossby wave, which was aroused by cyclonic wind stress, resulted in a westward shift of the subsurface cooling. This could be clearly seen in the CSP and ESP experiments (Figs. 1e and f). In the WSP experiment, the cooling was located within the forcing domain due to the western continental boundary (Fig. 1d).

The thermocline warming in the equatorward flank of forcing domains resulted from a similar mechanism. While subtropical SST forcing caused anomalous low pressure and cyclonic wind stress locally, it also led to anomalous westerlies and anomalous wind stress curl at its equatorward flank (Figs. 5a–c), and in turn downwelling at the bottom of the Ekman layer (Figs. 5d–f). The warm water from the bottom of the Ekman layer led to subsurface warming between the subtropical forcing domains and the equator (Figs. 1d–f). The zonal mean structure of the dipole-like temperature anomalies indicates clearly that the warming signal propagated equatorward from an off-equator thermocline warming center through the SEC and EUC, ultimately leading to a warming of the equatorial thermocline (Fig. 3).

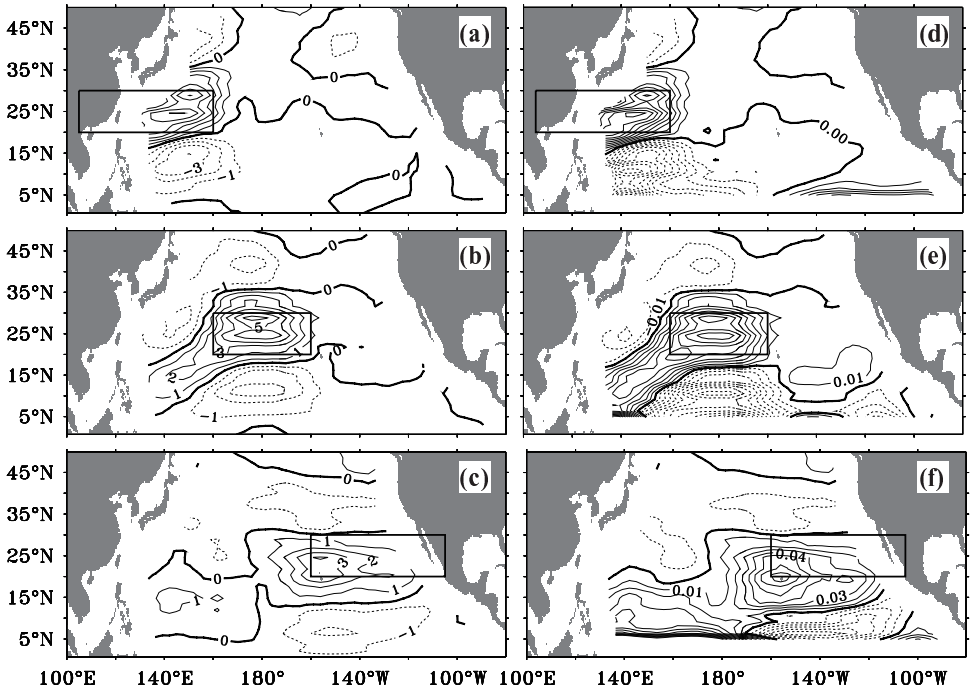

Fig. 5. Changes of wind stress curl (left panel; units: 10^{-8} N m^{-3}) and Ekman pumping (right panel; units: m d^{-1}) for the (a, d) WSP, (b, e) CSP, and (c, f) ESP experiments. The subtropical forcing domains are indicated by the solid line rectangular boxes.

From the above analysis, we can conclude that the "oceanic tunnel" only works in the process whereby warming propagates equatorward from the downwelling areas south of the forcing domains. Instead of affecting the equatorial Pacific through direct subtropical–equatorial water exchange, our results emphasize that the impact of the subtropics on the equatorial Pacific thermocline is an indirect, but much faster process, mainly depending on air–sea coupling.

4.2. *Changes in STCs*

Changes STCs also play a role in sustaining the equatorial thermocline warming. In all the experiments, the northern STC (NSTC) slowed down due to the weakening of eastern winds. This is consistent with previous studies that the strength of STCs depends on the strength of trade winds in both hemispheres (Nonaka et al., 2002; Yang et al., 2004). The weakened STCs suppressed the upwelling and reduced the poleward heat transport, warming the equatorial SST. The most significant weakening of the NSTC occurred in the ESP experiment (Fig. 6c), indicating the key region where the trade wind affects the Pacific NSTC the most. In the WSP and CSP experiments, we noticed that the anomalous NSTC was divided into two closed cells (Figs. 6a and b), which was related to strong Ekman downwelling around 8°N (Figs. 5d and e).

4.3. *Heat budget analysis*

To further understand the dynamic mechanisms of the responses in the equatorial thermocline to the subtropical North Pacific thermal forcing, the heat budget was analyzed by calculating term balances (see Appendix) within both the Pacific

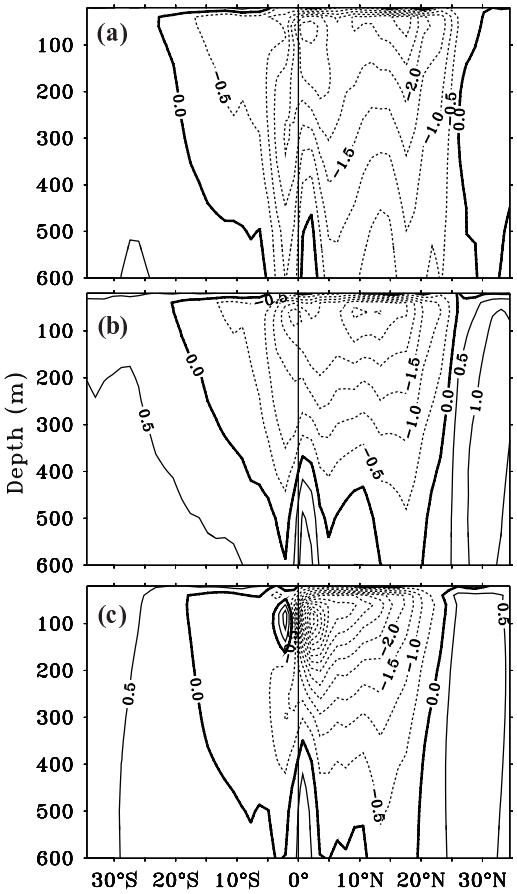

Fig. 6. Changes of the mean Pacific meridional overturning circulation in the (a) WSP, (b) CSP, and (c) ESP experiments (units: Sv). The vertical axis represents depth in the ocean (m).

equatorial thermocline (dashed line rectangular boxes in Figs. 1d–f) and the dipole-like temperature anomalies areas (red boxes and blue boxes in Fig. 7).

To investigate the warming mechanism in the equatorial thermocline, boxes were selected between 22.7 and 25.5 isopycnal levels (dashed line rectangular boxes in Fig. 1), within which the thermocline changes were most distinct (ultimately 0.32°C, 0.28°C, and 0.23°C, respectively; Fig. 2, green lines). To better understand the heat budget in the sensitivity experiments, the mean climatology of the term balance is also plotted. Usually, the equatorial thermocline (Figs. 8a–c) is maintained primarily by the warming effect of the heat transport from the extratropics (for north of the equator, $v < 0, T_y > 0$, and thus $-vT_y > 0$) and cooling effect of the cold-water upwelling ($w > 0, T_z > 0, -wT_z < 0$). The three sensitivity experiments (Figs. 8d–f) shared the feature that the equatorial thermocline was mainly warmed by the enhanced meridional advection. Both the perturbation meridional advection and mean meridional advection played a role in warming the equatorial thermocline. Take CSP for example: Within the selected box, on the one hand the perturbation meridional temperature gradient was positive (for the North Hemisphere, $T'_y > 0$; Fig. 1e); so, the mean equatorward current ($v < 0$) led to positive mean meridional advection ($-vT'_y > 0$; Fig. 8e, thin dark-grey bar), which represented heat transportation from the adjacent thermocline warming center. This term played a relatively important role in the WSP and ESP experiments (Figs. 8d and f, thin dark-grey bar). On the other hand, the mean meridional temperature gradient was negative in the Northern Hemisphere ($T_y < 0$); so, the anomalous poleward current ($v' > 0$, Fig. 6b) resulted in positive perturbation meridional advection ($-v'T_y > 0$; Fig. 8e, thin light-grey bar), and consequently a rise in temperature. This term represents enhanced equatorward heat transportation from off-equator by anomalous current, which played a relatively important role in the CSP experiment.

The term balance of the subtropical thermocline cooling and the off-equator warming were also calculated to further confirm the proposed mechanism. Take CSP for example: The most significant dipole-like warming and cooling (Fig. 1e) are indicated using the boxes in Fig. 7. For the corresponding CTRL, the mean climatology in the subtropical cooling box (Fig. 7, blue box) was mainly maintained by the balance between the warming effect of vertical and meridional temperature advections and the cooling effect of vertical diffusion and convection (Fig. 9a); whereas, in the off-equator warming box (Fig. 7, red box), it was maintained by the balance between the warming effect of vertical temperature advection and the cooling effect of meridional temperature advection and horizontal diffusion (Fig. 9b). Generally, $T_z > 0$ (Fig. 7a, colors) and $w < 0$ (Fig. 7b, contours) for both the boxes; thus, the vertical temperature advection warmed the subsurface ocean for both of them in the CTRL run. In the corresponding sensitivity experiment, CSP, the key role of vertical temperature advection was highlighted again for the anomalous term balance of both boxes, though playing opposite roles in the two boxes. Figure 9c indicates that the local subsurface cooling was caused by the weakened vertical

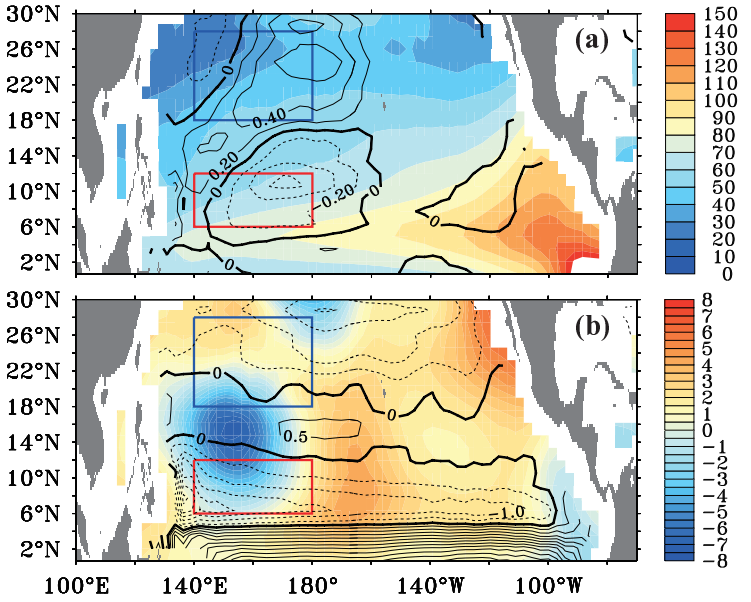

Fig. 7. (a) The thermocline mean vertical temperature gradient in the CTRL run (colors; units: 10^{-3}°C m^{-1}) with the thermocline upwelling changes in the CSP experiment (contours; units: 10^{-6} m s^{-1}) averaged between the 22.7 and 25.5 isopycnal levels. (b) The thermocline mean upwelling (contours; units: 10^{-6} m s^{-1}) in the CTRL run with the vertical temperature gradient changes in the CSP experiment (colors; units: 10^{-3}°C m^{-1}) averaged between the 22.7 and 25.5 isopycnal levels.

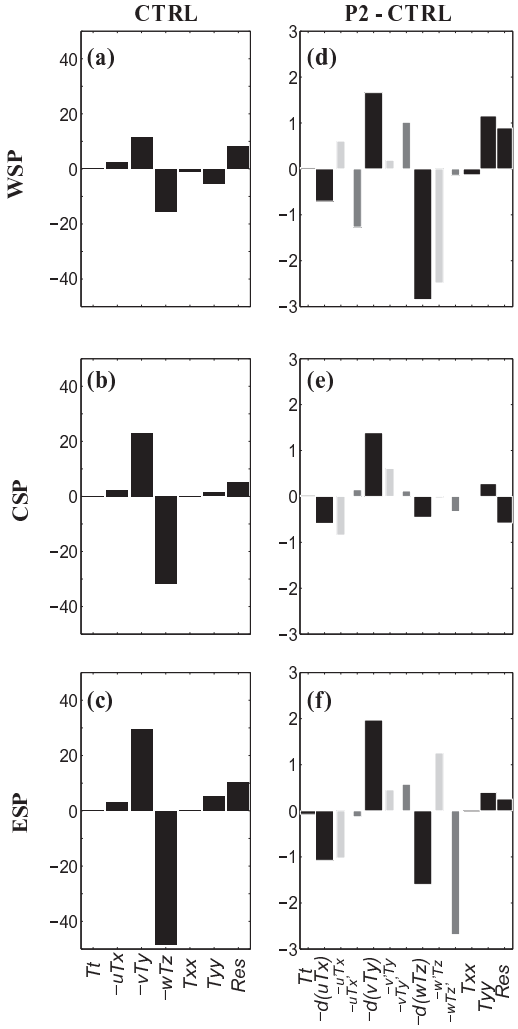

Fig. 8. The total term balance of the CTRLs (left panel) and their changes (right panel) for the (a, d) WSP, (b, e) CSP, and (c, f) ESP experiments calculated for the equatorial thermocline boxes (isopycnal level 22.7–25.5) indicated in Figs. 1d–f (dashed line rectangular boxes) [units: °C (10 yr)$^{-1}$]. The physical meaning of each bar is marked below the lower panel.

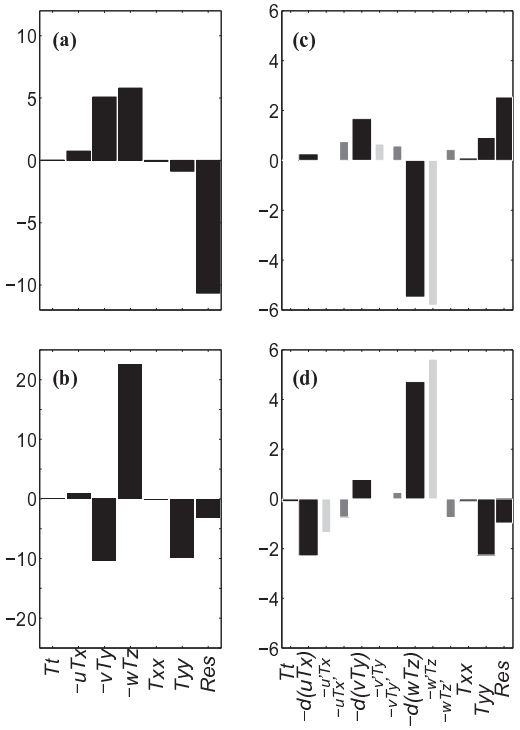

Fig. 9. The total term balance of the CTRLs (left panel) and their changes (right panel) for the (a, c) cooling center (Fig. 7, blue box) and (b, d) warming center (Fig. 7, red box) in the CSP experiment [units: °C (10 yr)$^{-1}$]. The physical meaning of each bar is marked below the lower panel.

temperature advections [$-\mathrm{d}(wT_z) < 0$]. Further decomposition of $-\mathrm{d}(wT_z)$ showed that the change was primarily caused by the weakened downwelling ($w' > 0$, Fig. 7a) and, consequently, a cooling effect of perturbation vertical temperature advection ($-w'T_z < 0$; Fig. 9c, thin light-grey bar), consistent with the weakening of northern STCs (Fig. 6b). In contrast, perturbation vertical temperature advection [$w' < 0, T_z > 0$ (Fig. 7a), so $-w'T_z > 0$ (Fig. 9d, thin light-grey bar)] caused the enhanced vertical temperature advection [$-\mathrm{d}(wT_z) > 0$], which increased the subsurface temperature in the warming box. This was also true in the WSP and ESP experiments. Anomalous winds caused by the subtropical SST forcing did not only generate positive wind stress curl anomalies in the forcing domains, but also led to anomalous negative wind stress curl to the north and south of the forcing domains (Figs. 5a–c). The anomalous vertical motions (Figs. 5d–f) aroused by the anomalous wind stress curl, which agreed well with the heat budget analysis (Fig. 9), are the most direct proof of the importance of air–sea coupling in the subtropical impact on the equatorial thermocline.

5. Conclusions and discussions

Using the so-called PC technique, the impact of the subtropical North Pacific on the equator was revisited using a fully coupled climate model. Not only the equatorial SST responses, but also the equatorial thermocline responses to the western, central and eastern subtropical North Pacific thermal forcing were found to be comparable.

The mechanism of equatorial thermocline warming was carefully investigated in this study. Instead of the water exchange pathway theory, which has been emphasized in many previous studies, we have highlighted an indirect, but much faster mechanism of the subtropical impact on the equatorial thermocline: namely, that the thermal forcing imposed on the subtropical North Pacific leads to an adjustment of wind stress in the low–mid latitudes (Figs. 5a–c), which results in anomalous oceanic upwelling near the forcing domains and downwelling in its equatorward flank (Figs. 5d–f). Both the anomalous upwelling and downwelling result in local temperature anomalies in the subsurface (Figs. 1d–f), with the latter dominating the equatorial thermocline warming.

In our previous work (Yang and Wang, 2008), the tropical ($< 30^\circ$) response to warmed and cooled extratropical SST were both investigated using the same model as we used in this study. It was found that the nonlinear response in the tropical upper ocean is less than 10% of the linear response to the extratropical SSTA. The insignificance of tropical nonlinear response is mainly due to the fact that the ocean circulation tends to change antisymmetrically in the warming and cooling experiments. Therefore, we expected general linearity in the equatorial response to the imposed subtropical forcing in this study. That is, anomalous downwelling was expected to occur in the local subsurface of the subtropical SST cooling forcing, while anomalous upwelling at its southern flank. The latter would produce thermocline cooling, propagating equatorward and resulting in cooling in the equatorial thermocline.

Our results demonstrated a much faster equatorial response. After the first 5 years, the response patterns resembled the final state very well (Figs. 4a–c), with the warming centers being exactly in the locations where they were in equilibrium stages (Figs. 4d–f). The responses during first 5 years reached more than 50% of that in equilibrium stages. In contrast, Matei et al. (2008) showed no warming to occur at the equator until 30 years of simulation, which was in accordance with decadal or even longer time scales of water exchange between the tropics and extratropics. Furthermore, Matei et al. (2008) emphasized the key role of the oceanic tunnel, by which only the water particles from the "subduction window" could reach the equatorial thermocline. Our model results, however, suggested that under the thermal forcing in the subtropics, air–sea coupling plays the dominant role in the equatorial thermocline changes, by which the "subduction window", as well as other longitude bands in the subtropical North Pacific, can all impact the equatorial thermocline climate, indirectly but quickly.

In our previous studies, the PC technique was used to investigate tropical–extratropical climate interaction (Yang and Liu, 2005; Yang and Wang, 2008; Yang and Wang, 2011). Using the same model and technique, we showed the vertical mean Pacific subsurface temperature changes of the forcing domains to exhibit the same sign as those of the exerted SST forcing in warmed/cooled extratropical ($> 30^\circ$) SST experiments. Accordingly, one important question here is: why did the subsurface changes of the forcing domains in the present study show the opposite sign to those of the surface forcing? In fact, both the subtropical and extratropical warmed (cooled) SST were able to locally generate the positive (negative) vertical temperature gradient, as well as positive (negative) wind stress curl, and in turn, the upwelling (downwelling) below the Ekman layer, which meant $T_z' > 0$ ($T_z' < 0$) and $w' > 0$ ($w' < 0$). Due to the mean positive vertical temperature gradient ($T_z > 0$) and mean downwelling ($w < 0$) in the subtropical and extratropical regions, the perturbation vertical temperature advection ($-w'T_z$) and the mean vertical temperature advection ($-wT_z' > 0$) should always be in opposite sign. Ekman pumping can be expressed as $W_E = -(\mathrm{curl}\boldsymbol{\tau})/\rho f - (\beta\tau_x)/(\rho f^2)$ (Shuto, 1996), where $\boldsymbol{\tau}$ is the vector wind stress, τ_x is zonal wind stress, ρ is density of the ocean, and f is the Coriolis parameter. It shows that, even forced by the same magnitude of wind stress, the aroused Ekman pumping is much stronger in lower latitudes than in higher latitudes due to the β-effect.

In the case of subtropical or extratropical SST warming, perturbation vertical temperature advection ($-w'T_z < 0$) and mean vertical temperature advection ($-wT_z' > 0$) always play an opposite role in local subsurface temperature changes. In our previous studies, in which the anomalous warmed SST was imposed poleward of 30°, the magnitude of w' was relatively small due to the largeness of the Coriolis parameter there. Thus, the magnitude of $-w'T_z$ was smaller than that of the $-wT_z'$, which resulted in a warmed subsurface. In the present study, however, the forcing domains (20°–30°N) were closer to the equator, so the anomalous wind stress could lead to much more intense upwelling due to the β-effect. As is shown in Fig. 9c, the magnitude of the perturbation vertical temperature advection $-w'T_z$ was so large that it dominated the anomalous vertical temperature advection $-d(wT_z)$ and made itself the dominant role in the subsurface cooling. The β-effect can also explain why the negative wind stress curl in the area to the south of the forcing domain (Figs. 5a–c), which was of comparable magnitude to that in the area to the north of the domain, generated much stronger downwelling than that in the area to the north (Figs. 5d–f).

Further investigation is needed for a deeper understanding of the relative significance between perturbation vertical temperature advection and mean vertical temperature advection to the local subsurface changes, and we intend to perform experiments with different magnitudes of subtropical forcing in order to further diagnose this.

Although it is uncertain if our results would also be valid in other models, this work is nevertheless valuable for its provision of a quantitative estimate of the equatorial responses to the subtropical North Pacific thermal forcing within different longitude bands. Instead of denying the water exchange pathways (e.g. oceanic tunnel) by which subtropical water particles penetrate into the equator, the message of this study is to remind people of the vital role of air–sea coupling, by which the "subduction window", as well as other longitude bands in the subtropical North Pacific, can all impact the equatorial thermocline climate, indirectly but effectively. We would also like to emphasize that surface thermal forcings in the low-mid latitudes should not be treated only as a "passive tracer", since the Coriolis effect might play a very important role there.

Acknowledgements. This work was jointly supported by the National Natural Science Foundation of China (Grant Nos. 40976007, 41176002, and 41376007), the National Basic Research Program of China (Grant No. 2012CB955201), the Special Fund for Meteorological Scientific Research in the Public Interest of the China Meteorological Administration (Grant No. GYHY201006022), the Specialized Research Fund for the Doctoral Program of Higher Education of China (2010), and the Special Fund for Environmental Protection Scientific Research in the Public In-

terest of the Ministry of Environmental Protection of the People's Republic of China (Grant No. 201309056) The authors benefited from the invaluable comments of the two anonymous reviewers. All the experiments were carried out on the supercomputer at Peking University.

APPENDIX A

Term Balance Analysis

The terms in the temperature equation are:

$$\partial T/\partial t = -uT_x - vT_y - wT_z + A_h T_{xx} + A_h T_{yy} + H + R\,. \quad \text{(A1)}$$

Here, $\partial T/\partial t$ represents the local temperature tendency; $-uT_x, -vT_y$ and $-wT_z$ represent the zonal, meridional and vertical temperature advection, respectively; $A_h T_{xx}$ and $A_h T_{yy}$ represent the horizontal diffusion terms with the constant diffusion coefficient A_h (4000 $m^2\ s^{-1}$); and H represents the surface net heat flux forcing (zero for the thermocline box). The vertical diffusion and convection are included in the R term. R is obtained by subtracting the other terms from $\partial T/\partial t$, because it cannot be directly calculated. The changes of all terms used in this paper are derived as the differences between the terms from the sensitivity PC experiments and their CTRLs. These anomalous terms are:

$$\partial T'/\partial t = -(uT_x)' - (vT_y)' - (wT_z)' + A_h T'_{xx} + A_h T'_{yy} + H' + R', \quad \text{(A2)}$$

where $\partial T'/\partial t = (\partial T/\partial t)_{PC} - (\partial T/\partial t)_{CTRL}$ and all other terms are similarly obtained. In this paper, the time average over the last 50-yr simulation is analyzed.

The temperature advection terms can be further decomposed as

$$\begin{cases} -(uT_x)' = -u'T_x - uT'_x - u'T'_x \\ -(vT_y)' = -v'T_y - vT'_y - v'T'_y \\ -(wT_z)' = -w'T_z - wT'_z - w'T'_z \end{cases}. \quad \text{(A3)}$$

Thus, the changes in the temperature advection result from the changes of mean current $(-u'T_x, -v'T_y, -w'T_z)$ and mean temperature gradient $(-uT'_x, -vT'_y, -wT'_z)$ as well as their nonlinear interactions $(-u'T'_x, -v'T'_y, -w'T'_z)$. The temperature gradient is positive poleward and upward. We do not discuss the nonlinear terms in this paper, since they are usually so small that they can be safely discarded.

REFERENCES

Coles, V. J., and M. M. Rienecker, 2001: North Pacific subtropical-tropical gyre exchanges in the thermocline: Simulations with two isopycnic OGCMs. *J. Phys. Oceanogr.*, **31**, 2590–2611.

Gu, D., and S. G. H. Philander, 1997: Interdecadal climate fluctuations that depend on exchanges between the Tropics and extratropics. *Science*, **275**, 805–807.

Huang, B. Y., and Z. Y. Liu, 1999: Pacific subtropical-tropical thermocline water exchange in the National Centers for Environmental Prediction ocean model. *J. Geophys. Res.*, **104**, 11 065–11 076.

Huang, R. X., and Q. Wang, 2001: Interior communication from the subtropical to the tropical oceans. *J. Phys. Oceanogr.*, **31**, 3538–3500.

Jacob, R., 1997: Low frequency variability in a simulated atmosphere ocean system. Ph. D. thesis, University of Wisconsin-Madison, 159 pp.

Kerr, R. A., 2004: Three degrees of consensus. *Science*, **305**, 932–934.

Lee, T., and I. Fukumori, 2003: Interannual-to-decadal variations of tropical-subtropical exchange in the Pacific Ocean: Boundary versus interior pycnocline transports. *J. Climate*, **16**, 4022–4042.

Liu, Z., S. G. H. Philander, and R. C. Pacanowski, 1994: A GCM study of tropical-subtropical upper-ocean water exchange. *J. Phys. Oceanogr.*, **24**, 2606–2623.

Luo, Y. Y., L. M. Rothstein, and R.-H. Zhang, 2009: Response of Pacific subtropical-tropical thermocline water pathways and transports to global warming. *Geophys. Res. Lett.*, **36**, L04601, doi: 10.1029/2008GL036705.

Matei, D., N. Keenlyside, M. Latif, and J. Jungclaus, 2008: Subtropical forcing of tropical Pacific climate and decadal ENSO modulation. *J. Climate*, **15**, 4691–4709.

McCreary, J. P., and P. Lu, 1994: Interaction between the subtropical and equatorial ocean circulations: The subtropical cell. *J. Phys. Oceanogr.*, **24**, 466–497.

McPhaden, M. J., and R. A. Fine, 1988: A dynamical interpretation of the tritium maximum in the central equatorial Pacific. *J. Phys. Oceanogr.*, **18**, 1454–1457.

Nonaka, M., S.-P. Xie, and J. P. McCreary, 2002: Decadal variations in the subtropical cells and equatorial Pacific SST. *Geophys. Res. Lett.*, **29**(7), 1116, doi: 10.1029/2001GL013717.

Rothstein, L. M., R.-H. Zhang, A. J. Busalacchi, and D. Chen, 1998: A numerical simulation of the mean water pathways in the subtropical and tropical Pacific Ocean. *J. Phys. Oceanogr.*, **28**, 322–343.

Shuto, K., 1996: Interannual variations of water temperature and salinity along the 137°E meridian. *J. Oceanogr.*, **52**, 575–595.

Wang, L., and H. J. Yang, 2013: Impact of subtropical pacific SSTA on the Equatorial Ocean. *Acta Scientiarum Naturalium Universitatis Pekinensis*, **49**, 791–798.

Wang, Q., and R. X. Huang, 2005: Decadal variability of pycnocline flows from the subtropical to the equatorial Pacific. *J. Phys. Oceanogr.*, **35**, 1861–1875.

Yang, H. J., and L. Wang, 2008: Estimating the nonlinear response of tropical ocean to extratropical forcing in a coupled climate model. *Geophys. Res. Lett.*, **35**, L15705, doi: 10.1029/2008GL034256.

Yang, H. J., and L. Wang, 2011: Tropical oceanic response to extratropical thermal forcing in a coupled climate model: a comparison between the Atlantic and Pacific oceans. *J. Climate*, **24**, 3850–3866.

Yang, H. J., and Z. Y. Liu, 2005: Tropical-extratropical climate interaction as revealed in idealized coupled climate model experiments. *Climate Dyn.*, **24**, 863–879.

Yang, H. J., Z. Y. Liu, and H. Wang, 2004: Influence of extratropical thermal and wind forcings on equatorial thermocline in an ocean GCM. *J. Phys. Oceanogr.*, **34**, 174–187.